Available online at www.sciencedirect.com
SCIENCE DIRECT®
Physics and Chemistry of the Earth 29 (2004) 473–480
PHYSICS and CHEMISTRY of the EARTH
www.elsevier.com/locate/pce

Critical dynamics of fractal fault systems and its role in the generation of pre-seismic electromagnetic emissions

V. Uritsky [a,*], N. Smirnova [a], V. Troyan [a], F. Vallianatos [b]

[a] *Institute of Physics, St. Petersburg University, St. Petersburg 198504, Russia*
[b] *Technological Educational Institute of Crete, Chania 73133, Crete, Greece*

Received 20 July 2003; received in revised form 27 November 2003; accepted 28 November 2003
Available online 2 April 2004

Abstract

Regional seismicity is known to demonstrate scale-invariant properties in different ways. Some typical examples are fractal spatial distributions of hypocenters, Gutenberg–Richter magnitude statistics, fractal clustering of earthquake onset times, power-law decay of aftershock sequences, as well as scale-invariant geometry of fault systems. In some regions, the observed scale-free effects are likely to be connected to a cooperative behavior of interacting tectonic plates and can be described in terms of the self-organized criticality (SOC) concept. In this work, we investigate a new SOC model incorporating short-term fractal dynamics of seismic instabilities and slowly evolving matrix of cracks (faults) reflecting long-term history of preceding events. The model is based on a non-Abelian directed sandpile algorithm proposed recently by Hughes and Paczuski [Phys. Rev. Lett. 88 (5), 054302-1], and displays a self-organizing fractal network of occupied grid sites similar to the structure of stress fields in seismic active regions. Depending on the geometry of local stress distribution, some places on the model grid have higher probability of major events compared to the others. This dependence makes it possible to consider a time-dependent structure of the background earth crust geometry as a sensitive seismic risk indicator. We also propose a simple framework for modeling ultra-low frequency (ULF) electromagnetic emissions associated with abrupt changes in the large-scale geometry of the stress distribution before characteristic seismic events.

1. Introduction

The concept of self-organized criticality (SOC) (Bak et al., 1987, 1988) provides a promising framework for modeling and interpreting scale-invariant patterns in nature (Takayasu, 1990). Various SOC models have been successfully applied for describing Gutenberg–Richter earthquake magnitude statistics and explaining its universal features (Turcotte, 1999). Most of the developed SOC models of distributed seismicity are concentrated on the dynamics of scale-free avalanches (discrete energy release events) considered as a model for earthquakes. However, although the avalanches involve many spatial degrees of freedom, they do not normally lead to an emergence of large-scale spatial correlations over periods of time longer than a lifetime of a single avalanche. As a result, SOC models turned out to be unable to explain fractal clustering of earthquake hypocenters and their relation to the evolution of fault systems which seem to play an important part in real seismic systems (Pavlides et al., 1999). Several attempts have been made to introduce pre-defined (quenched) fault matrixes in SOC simulations, but until recently, none of the developed models could mimic the dynamical coupling that exists between slowly evolving fault structures and seismic instabilities.

The first SOC model that successfully incorporated scale-free avalanche activity with a fault matrix dynamics has been presented in Hughes and Paczuski (2002). The key component of this model is the absence of the Abelian symmetry (Dhar, 1999). If the Abelian symmetry is violated, the avalanches begin to rearrange modal landscape in such a way that spatial distribution of close to instability threshold grid sites becomes strongly non-uniform, which creates a complex fractal network of preferred paths for propagation of future avalanches. In contrast to previous SOC models, the emerging spatial pattern is not static; it evolves slowly in accordance with the avalanche dynamics keeping the entire system in the vicinity of global critical point

* Corresponding author.
E-mail address: uritsky@geo.phys.spbu.ru (V. Uritsky).

1474-7065/$ - see front matter © 2004 Elsevier Ltd. All rights reserved.
doi:10.1016/j.pce.2003.11.015

manifesting itself in power-law avalanche distributions over energy, size and lifetime.

In the present work, we investigate the non-trivial spatial structure of the Hughes and Paczuski model, and propose a simple framework for modeling ultra-low frequency (ULF) electromagnetic emission signals associated with abrupt changes in the large-scale geometry of stress distribution before characteristic seismic events.

2. Model description

The model is defined on a two-dimensional grid (Fig. 1). Each grid site is prescribed the integer-valued coordinates $x = 0, \ldots, N_x - 1$ and $y = 0, \ldots, N_y - 1$, as well as the state variable $z(x, y)$ arbitrarily called energy. The amount of energy stored in a given element determines its ability to interact with other elements. In our study, we used a real-valued modification of the Hughes and Paczuski (HP) sandpile algorithm (Hughes and Paczuski, 2002) with $z \in R$. When at any site the variable z exceeds constant instability threshold ($z > z_c$) it "topples" transferring certain amount of its energy to downstream nearest neighbors:

$$\begin{aligned} z_{t+1}(x, y) &= z_t(x, y) - \mathrm{d}z, \\ z_{t+1}(x+1, y+1) &= z_t(x+1, y+1) + p\,\mathrm{d}z, \\ z_{t+1}(x, y+1) &= z_t(x, y+1) + (1-p)\,\mathrm{d}z, \end{aligned} \tag{1}$$

in which t is discrete time and $p \in [0, 1]$ is a uniformly distributed random variable updated each time the interaction rules (1) are applied. After receiving a portion of energy from the excited element, one or two of its downstream nearest neighbors can also go unstable producing a growing avalanche of activity that propagates along the y-direction. The avalanche stops when its front reaches "cold" grid sites whose z values are low enough to absorb the energy from the unstable elements without producing new activity, or when it reaches the open bottom boundary at $y = N_y - 1$. The left and right edges of the grid are subject to the periodic boundary condition $z(0, y) \equiv z(N_x - 1, y)$.

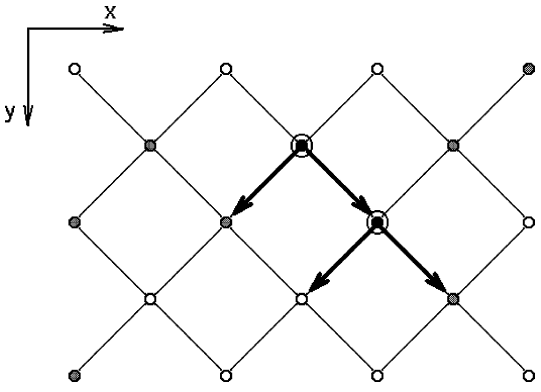

Fig. 1. A sketch illustrating the interaction rules in 2-D HP sandpile model (Hughes and Paczuski, 2002). Active grid sites ($z > z_c$) marked with large open circles interact with downstream nearest neighbors which can produce further activity provided their energy before the interaction exceeds the level $z_c - \mathrm{d}z$ (dashed circles).

The model is driven by adding a small amount h of energy to randomly chosen sites on the top row ($y = 0$) until the condition $z > z_c$ is fulfilled and an instability is initiated in some site. During the subsequent avalanche propagation, the driving is suspended which provides infinite separation between the driving and the avalanche time scales necessary for SOC in sandpile-type models (Vespignani and Zapperi, 1998). In our calculations we used the following set of the model parameters: $N_x = N_y = 400$, $h = 1$, $z_c = 1$. Parameter $\mathrm{d}z$, the energy transferred by an unstable grid site, was chosen as described in the next section.

After a transient period, the model reaches the SOC state at which the probability distributions of avalanches over size s and lifetime t are given by

$$\begin{aligned} p(s) &= s^{-\tau_s} f(s/s_c), \\ p(t) &= t^{-\tau_t} g(t/t_c), \end{aligned} \tag{2}$$

where f and g are appropriate scaling functions controlling the cutoff behavior of the distributions, s_c and t_c are finite-size scaling parameters, and τ_s and τ_t are the avalanche scaling exponents.

In general, the scale-free avalanche statistics (2) does not necessarily imply any significant correlations between spatially separated grid sites over time scales exceeding avalanche lifetimes. Typically, stochastic sandpile models never exhibit such correlations which means that spatial distribution of grid energy $z(x, y)$ between the avalanches is effectively random. In this context, the HP model presents a new opportunity to study the emergence of non-trivial large-scale structures appearing self-consistently in the SOC state.

3. Abelian versus non-Abelian dynamics of the HP model

The key parameter in the HP model that controls large-scale correlations in $z(x, y)$ is $\mathrm{d}z$, the fraction of energy that is redistributed in local interactions (1). Keeping the value of $\mathrm{d}z$ constant and independent of z makes the sandpile algorithm Abelian (Dhar, 1999) and eliminates any spatial structures. On the contrary, setting $\mathrm{d}z$ to the current value of energy $z_t(x, y)$ at each point makes the algorithm non-Abelian and, as shown by Hughes and Paczuski (2002), leads to the emergence of complex spatial patterns.

Fig. 2 illustrates the difference between the behavior of the HP model in the Abelian and non-Abelian regimes. As one can see, spatial distribution of energy stored by subcritical grid sites with $z \leqslant z_c$ differs dramatically in these regimes. In the Abelian case, the

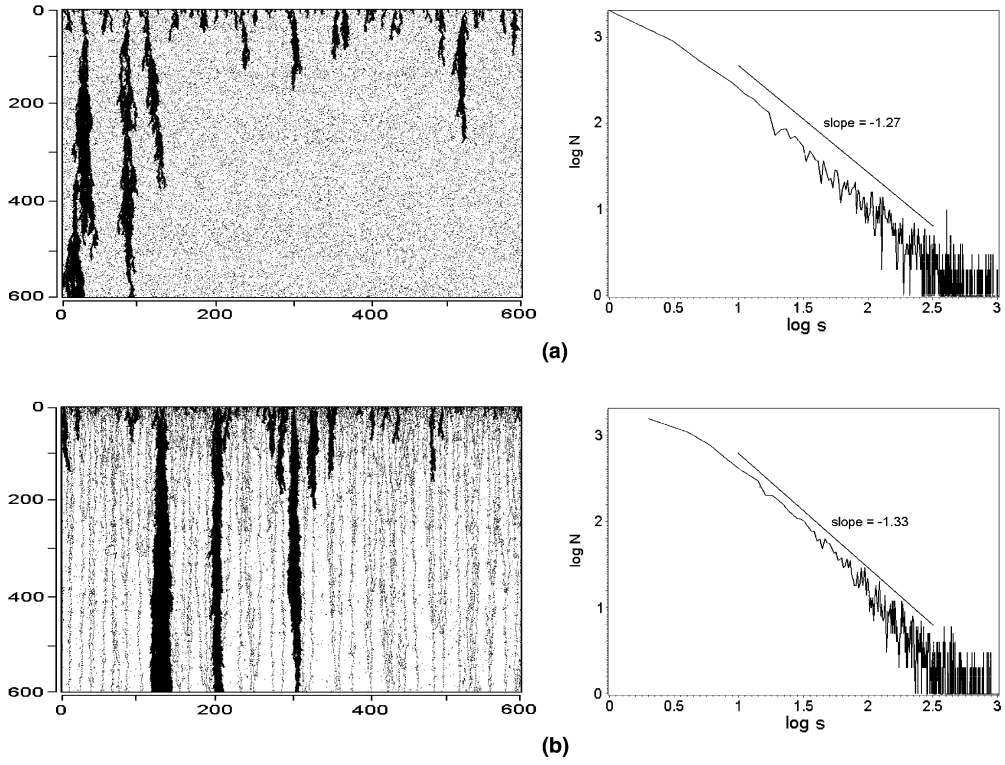

Fig. 2. Typical spatial patterns of occupied grid sites (left) and avalanche-size probability distributions (right) in the Abelian (a) and non-Abelian (b) versions of the HP model.

model has effectively no correlations in space; in the non-Abelian case, it shows distinct multiscale structures constituting a branching network of interconnected elements. Despite this dramatic difference, avalanche size probability distributions are nearly identical and follow power-law relations signaling that the model reaches the SOC state in both regimes, and that the dynamics of excited grid elements on the time scale of individual instabilities are strongly correlated in both cases.

To study the emergence of non-trivial large-scale correlations in the non-Abelian HP model, we have evaluated the entropy characterizing spatial disorder of subcritical grid sites as a function of spatial scale. The simulation grid was divided into square boxes of linear size l, for which mean values $\bar{z}$ of energy were calculated at every time step (i.e. after every avalanche). The degree of disorder associated with non-uniform energy distribution can then be characterized by the information entropy

$$S(l) = -\int_0^\infty p_l(\bar{z}) \log_2 p_l(\bar{z})\, \mathrm{d}\bar{z} \quad \text{(bits)}, \tag{3}$$

where $p_l(\bar{z})$ is the probability distribution of $\bar{z}$ at the spatial scale l. Assuming that $\bar{z}$ is a Gaussian variable, which seems to be the case when the boxes include large enough number of elements, formula (3) is approximated by

$$S(l) \approx \frac{1}{2} \log_2(2\pi e \sigma_l^2), \tag{4}$$

where σ_l is the standard deviation of $\bar{z}$ values in different boxes of the same size l. In the Abelian model with z randomly distributed over spatial locations, σ_l is proportional to $l^{-d/2}$, where d is the grid dimension, and therefore $S(l)$ should scale as

$$S \propto -\frac{d}{2} \log_2(l) = -\frac{d}{2 \log_{10} 2} \log_{10}(l). \tag{5}$$

Physically, it means that for large l, spatial fluctuations of energy are "averaged out" and become negligibly small. In the non-Abelian HP model possessing large-range spatial correlations the $S(l)$ should decay much slower because the increase in size of counting boxes does not guarantee in this case that spatial behavior of the coarse-grained energy field becomes more uniform.

The comparison between the scaling of entropy in the discussed regimes is shown in Fig. 3a. As one can see, S decreases with the box size l much faster in the Abelian case. On a semi-logarithmic plot, this dependence contains a straight-line segment with the slope predicted by Eq. (5). In the non-Abelian case, the entropy decays considerably slower, so that for large l it exceeds the entropy of the Abelian model by several orders of magnitude. The emergence of large-scale structures in

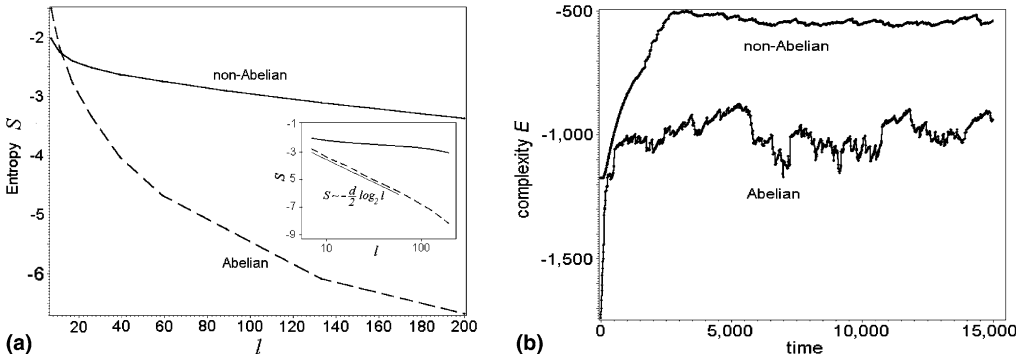

Fig. 3. (a) Entropy S characterizing spatial distribution of subcritical elements in Abelian and non-Abelian HP models ($N_x = N_y = 400$) as a function of linear box size l. (b) Dynamics of the complexity E accompanying evolution of the models towards stationary SOC state.

the non-Abelian HP sandpile is a direct result of its self-organization towards the SOC state. To illustrate this effect, we have studied the evolution of this sandpile starting from random initial conditions with z distributed uniformly over x and y and having the same average density as in the final SOC state.

The scaling of entropy in the initial state was nearly the same as in the final stationary state of the Abelian HP model. However, as the non-Abelian model approaches SOC, the large-scale structure in the spatial distribution of energy begins to appear leading to accumulation of "excess" entropy at large l. This process can be conveniently described by the evolution of the complexity measure

$$E(t) = \int_{l_{\min}}^{l_{\max}} S(l,t)\,\mathrm{d}l \tag{6}$$

representing the total amount of entropy within the range of the available spatial scales. Our simulations show a steady increase in the complexity as the non-Abelian model passes through its initial transient regime (Fig. 3b) and reaches SOC. In the SOC state, its complexity becomes nearly constant and exceeds complexity in the Abelian case.

4. Avalanche size and complexity of the fault structure

In what follows, we consider non-Abelian HP sandpile as a toy model of fractal fault system. Indeed, the scale-invariant spatial structure of interconnected subcritical regions in this model is formed by its preceding avalanche activity, similar to fractal fault systems being formed by earthquakes. Avalanches change the fractal network of sub-critical grid sites slowly, just as earthquakes modify the fault configuration slowly. In both cases, on a time scale of several events it may appear that the underlying spatial pattern is static, but in fact it is dynamic and reflects the prehistory of preceding instability events. In the steady state of the HP model, the fractal fault structure seems to be necessary for SOC avalanches to occur. Due to the power law decay of the probability of avalanches (2), the model can produce system-wide instabilities corresponding to large seismic events.

It should be noted that in real seismic systems, there are other factors than the earthquakes that form the structure of tectonic faults. The influence of such factors can drive the system out of exact SOC state distorting scale-invariant correlations and reducing or increasing the probability of system-wide events. Theoretically, this effect implies a possibility of predicting catastrophic earthquakes based on an analysis of fractal fault structure. In particular, one can expect that the average size of avalanches should decrease when the scale-invariant network of faults formed during the evolution of the system towards the SOC state is affected by random perturbations. To study numerically this dependence, we have evaluated average size $\overline{S}$ of avalanches produced by several sample grid configurations $z(x,y)$ in steady SOC state. Each configuration has been saved to the computer memory after which energy values of the k percent of randomly chosen pairs of grid sites have been swapped so that the long-range spatial correlations have been partly destroyed, and the E value of the randomized grid has been obtained. To determine $\overline{S}$, a unit energy has been added in succession to each of N_x elements of the top row ($y = 0$), and the sizes of the resulting avalanches have been recorded, with the initial grid configuration having been recovered from the memory after every avalanche. $\overline{S}$ has then been estimated by averaging over all the N_x events observed for this configuration.

Fig. 4 displays a relation between the spatial complexity E and the average avalanche size $\overline{S}$ obtained by this procedure for a typical steady state of the non-Abelian SP model. Most typically, E gradually decreases with k until about 60% of model elements are affected by random shuffling. The observed dependence is conditioned by the gradual loss of large-scale correlations between the states of grid elements due to the randomization. As Fig. 4 shows, the avalanche size $\overline{S}$ grows dramatically as the spatial complexity increases. Comparing $\overline{S}$ values in the pure SOC state with the highest

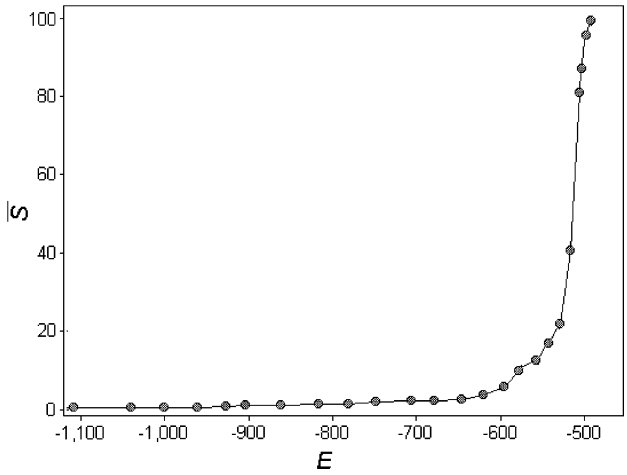

Fig. 4. Dependence of the average avalanche size on the complexity of the distribution of subcritical grid sites in a steady state of the non-Abelian HP model.

complexity and in the deeply randomized state ($E = -1200$), we have found that $\overline{S}$ differs by more than two orders of magnitude in these states. The largest value of $\overline{S}$ presented in this plot corresponds to $k = 0$ and is associated with the largest risk of system-wide instabilities. At lower E values, the average avalanche size becomes smaller, and so does the risk of system-wide catastrophic events.

The observed dependence strongly suggests that the average size of avalanches that can occur on a specific grid configuration can be predicted based on its spatial complexity. The estimated $\overline{S}$ value can then be used as a measure of system's response to week external perturbations (Vespignani and Zapperi, 1998). Assuming that the stress in the earth crust is accumulated at a slow steady rate, this method provides an opportunity of estimating seismic hazard level based on the complexity evaluation of a multiscale fault structure in the area of study.

5. Modeling conductivity fluctuations

The evolving spatial fractal fault structure discussed above can generate temporal signals that carry information on its configuration. This possibility is based on the fact that in the non-Abelian HP model, the probability of large events seems to depend on the distribution of energy at different spatial scales. The elements whose z values are close to the instability threshold tend to compose irregular branching "chains" able to channel activity throughout the grid and thus defining most probable paths for future avalanches. If an avalanche starts at a long chain of interconnected subcritical sites it has more chances to become a system-wide characteristic event compared to an avalanche initiated at a shorter chain.

By assuming that different energy levels of grid elements correspond to different values of electric conductivity, one can try to characterize the status of the fault system based on electric field measurements and estimate the associated seismic risk. We have constructed time series of electric conductivity of the model postulating that stable ($z = 0$) and subcritical ($0 < z \leqslant z_c$) grid sited symbolize respectively two different phases in the earth crust, e.g. solid rocks and fluids filling up cracks in the rocks (Tsunogai and Wakita, 1995). For the sake of simplicity, the conductivity of stable sites was set to zero and the conductivity of subcritical sites was set to 1. Consequently, the average concentration of the conducting phase in the spatial domain Ω of interest is

$$C(t) = \langle \theta(1 - z_t(x,y)) \rangle_{x,y\in\Omega} \tag{7}$$

in which $\langle\ \rangle_{x,y\in\Omega}$ denotes averaging over all the positions within Ω and θ is the Heaviside step function defined as $\theta(\xi \geqslant 0) = 1,\ \theta(\xi < 0) = 0$. The bulk (effective) conductivity of a disordered mixture conducting material — dielectric just above the percolation threshold C_0 is known to scale as $(C - C_0)^{\mu}$ with the critical exponent $\mu > 1$ (Bunde and Havlin, 1996). For correct estimation of the bulk conductivity based on this relation one needs to know the specific values of the parameters μ and C_0 which in case of the HP model should be sensitive to higher-order large-scale correlations in spatial distribution of z. Instead of investigating this dependence, we have evaluated the percolation conductivity σ_{p} from direct numerical simulations that allowed us to determine the connectivity of conducting grid sites in the studied region as a function of time. We assumed that the electric field is parallel to x-direction of the grid and is created by a constant external potential drop applied to the domain Ω. Under this condition, the electric current through Ω depends on the existence of a percolation cluster $\Pi \subset \Omega$ of subcritical grid sites connecting left and right boundaries of Ω. For the periods of time when such a cluster does exist the percolation conductivity can be calculated as follows:

$$\sigma_{\mathrm{p}}(t) = \left(\sum_{x\in\Omega} \left(\sum_{y\in\Omega} [Q(x,y) \times \theta(1 - z_t(x,y))] \right)^{-1} \right)^{-1},$$
$$Q(x,y) = \begin{cases} 1 & (x,y) \in \Pi, \\ 0 & (x,y) \notin \Pi. \end{cases} \tag{8}$$

For any other periods $\sigma_{\mathrm{p}} \equiv 0$. Formula (8) can be considered as an upper estimate for the total conductivity of the percolation cluster Π in which we neglect possible "dead-ends" and other topological structures not able to convey the electric current. This approximation turns out to be acceptable when the vertical size of the studied region is relatively small as it was in our simulation.

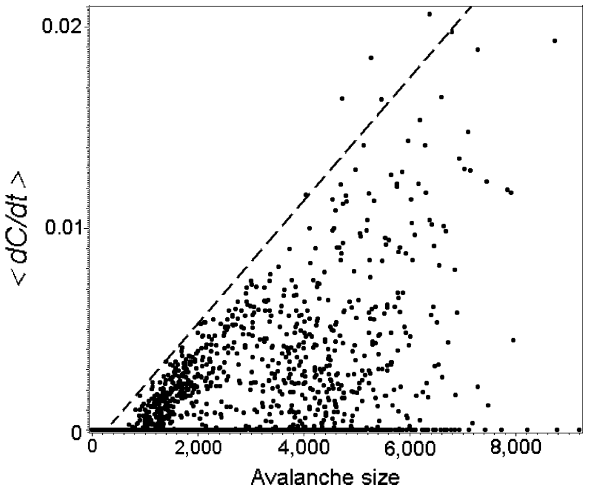

Fig. 5. Time derivative dC/dt of concentration fluctuations in the spatial domain $x = 50, \ldots, 150$; $y = 200, \ldots, 400$ averaged over lifetime of each avalanche, versus avalanche size.

The electric connectivity controlling σ_p plays an important part in fractal disordered materials (Bahr, 1997) and so can influence the generation of pre-seismic ULF electromagnetic signals. To model this effect, we have studied time series of concentration and conductivity fluctuations as defined by Eqs. (7) and (8), as well as the time series dC/dt and $d\sigma_p/dt$ of temporal derivatives of these signals. The derivatives turned out to be closely connected with the size of SOC avalanches reflecting the fact that the larger is the avalanche, the more pronounced is the change that it may cause in the spatial distribution of subcritical grid sites. This suggests that, by predicting time evolution of conductivity increments, one can estimate the maximum size of avalanches expected at future time instants (Fig. 5). To explore the possibility of such prediction, we have applied the detrended fluctuation analysis (DFA) technique (Stanley, 2003) allowing to identify weak correlations in scale-free stochastic processes. The DFA technique consists in the calculation of the mean-square deviation F of the time-integrated signal from its local linear regression fits over time intervals with different length τ, and estimating the power law exponent in the relation $F \sim \tau^{\alpha}$ that is detected in the range of τ where the studied signal is fractal. The power-law exponent α equals 1.5 when the signal is a Brownian-like process with uncorrelated time increments, and becomes greater or smaller than 1.5 if its time increments are positively or negatively correlated.

The analysis has shown that the concentration fluctuations have a broad-band fractal structure with the DFA exponent $\alpha = 1.5$ (Fig. 6a). This α value rules out the possibility of using the dependence between the time derivative dC/dt and the avalanche sizes for forecasting model's dynamics. In contrast, the DFA signature of the percolation conductivity is more complex and displays α

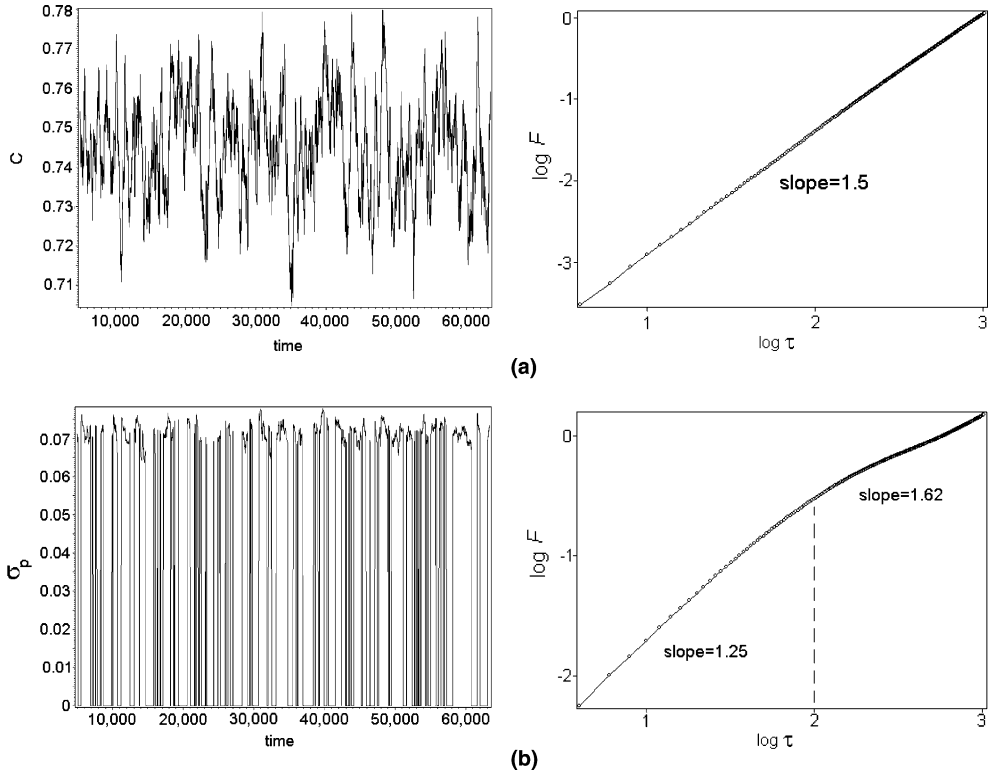

Fig. 6. Examples of temporal fluctuations (left) and the corresponding DFA functions (right) of concentration (a) and percolation conductivity (b) fluctuations estimated within the spatial domain $x = 0, \ldots, 200$; $y = 20, \ldots, 40$.

values that are significantly smaller or greater than 1.5 depending on the range of time scales of interest (Fig. 6b). For time scales shorter than the crossover time $\tau_c \simeq 10^2$, the DFA exponent is 1.25 ± 0.01, whereas for longer τ it takes on the value 1.62 ± 0.02. This scaling behavior indicates that the values of the time derivative of the percolation conductivity are correlated negatively at time scales $\tau < \tau_c$ but correlated positively at $\tau > \tau_c$. In both τ ranges, one can make certain statistical predictions regarding the sign and the value of $\mathrm{d}\sigma_p/\mathrm{d}t$ based on an analysis of preceding dynamics of this parameter, and on this basis estimate the probability of large avalanches expected in future.

6. Concluding remarks

We have briefly discussed the possibility of using the non-Abelian sandpile model due to Hughes and Paczuski (2002) for studying coupling effects between seismic activity and the multiscale spatial structure of faults. The principal advantage of the HP algorithm is its long-range spatial correlations that are not present in standard sandpile models of earthquakes. We have proposed an appropriate complexity measure allowing to quantify the emergence of non-trivial large-scale fault patterns in the SOC state of the model. The complexity seems to control the sensitivity of the model to small perturbations as well as the average size of avalanches, which provides an opportunity of building a predictive scheme for strong seismic events based on a multiscale analysis of the fault's fractal geometric structure.

We have also shown that the multiscale spatial behavior of subcritical energy distribution in the HP model manifests itself in fractal dynamics of the parameters defined by Eqs. (7) and (8). The conductivity fluctuations $\sigma_p(t)$ that allow for changeable percolation features of the fault matrix exhibit long-range correlations that can be used for the assessment of the range of avalanche sizes consistent with the current state of the system. The $\mathrm{d}\sigma_p(t)/\mathrm{d}t$ signal generated by unstable grid sites has distinct fractal properties. By its shape, this signal is reminiscent of pre-seismic ULF electromagnetic emissions that also display a clustering of activity before strong earthquakes (Fig. 7). However, a more elaborate version of the model should be created that includes specific electromagnetic parameters of the earth crust before its dynamics can be compared to the ULF emission in a quantitative way. Such a model should also be able to reproduce consecutive earthquake cycles with large events tending to recur on the same main fault(s), as it happens typically in real seismic systems (Tzanis and Vallianatos, 2003). This implies a non-trivial interplay between high-dimensional behavior associated with SOC mechanism and low-dimensional behavior due to reversible deviations of the fault matrix from its global critical point predicted by the concept of dynamical self-organization (Rundle et al., 2000). One way to combine these two mechanisms is to introduce certain amount of "static" memory into a sandpile

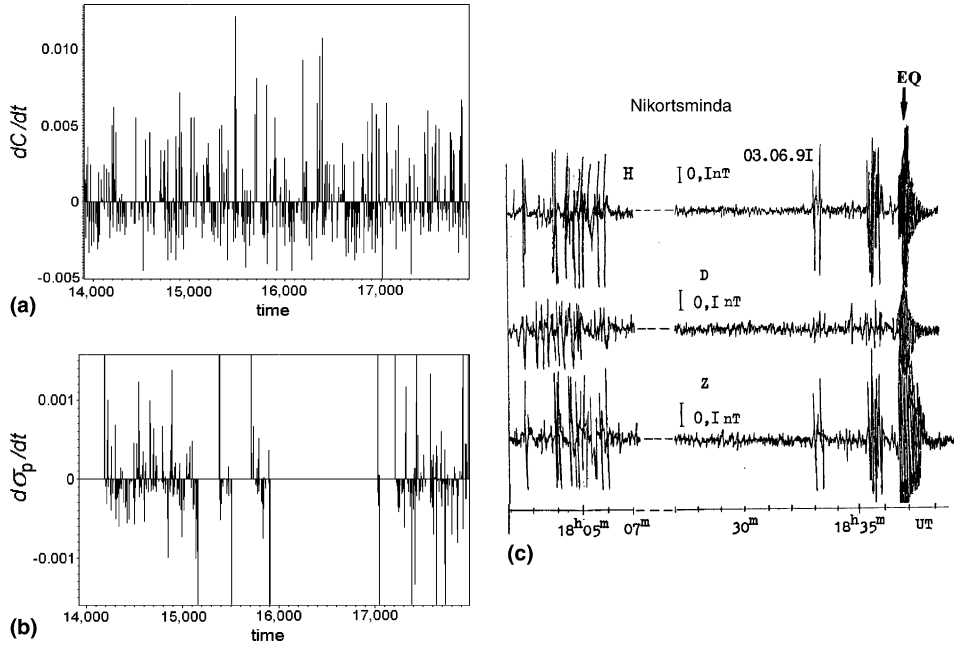

Fig. 7. Time evolution of signals $C(t)/\mathrm{d}t$ and $\mathrm{d}\sigma_p/\mathrm{d}t$ in the domain $x = 0, \ldots, 200$ as compared to ULF lithospheric emissions registered prior to the moderate ($M = 4$) Racha aftershock of 3 June 1991 (marked as EQ) with the observation point (Nikortsminda station) located about 40 km from the epicenter (Kopytenko et al., 1994) (c).

algorithm that would allow to mimic fault systems with quenched heterogeneities that survive many system-wide avalanches and define preferred locations for future catastrophic events. Another possible approach is to make the instability threshold z_c depending on large-scale properties of the model and/or the driver. Such a feedback leads naturally to low-dimensional loading-unloading cycle during which the system undergoes a transition from supercritical to subcritical global behavior without losing its scale-free features at small spatial and temporal scales (Uritsky et al., 2001). This effect may also play a significant part in the generation of seismic cycles and can be used for earthquake prediction.

Acknowledgements

The authors thank Dr. M. Paczuski for her valuable advice on the HP model, and Dr. A. Tzanis and another referee for useful comments and suggestions on the manuscript. The work was supported by INTAS grant 99–1102 and the *Intergeophysica* Russian research program.

References

Bahr, K., 1997. Electrical anisotropy and conductivity distribution function of fractal networks and of the crust: the scale effect of connectivity. Geophysical Journal International 130, 649–660.

Bak, P., Tang, C., Wiesenfeld, K., 1987. Self-organized criticality — an explanation of $1/F$ noise. Physical Review Letters 59 (4), 381–384.

Bak, P., Tang, C., Wiesenfeld, K., 1988. Self-organized criticality. Physical Review A 38 (1), 364–374.

Bunde, A., Havlin, S. (Eds.), 1996. Fractals and Disordered Systems. Springer, Berlin. 408pp.

Dhar, D., 1999. The Abelian sandpile and related models. Physica A 263 (1–4), 4–25.

Hughes, D., Paczuski, M., 2002. Large scale structures, symmetry, and universality in sandpiles. Physical Review Letters 88 (5), 054302-1–054302-4.

Kopytenko, Y.A., Matiashvili, T.G., Voronov, P.M., Kopytenko, E.A., 1994. Observation of electromagnetic ultra-low-frequency lithospheric emissions (ULE) in the Caucasian seismically active area and their connection with the Earthquakes. In: Hayakawa, M., Fujinawa, Y. (Eds.), Electromagnetic Phenomena Related to Earthquake Prediction. Terra Sci. Pub. Co., Tokyo, pp. 175–180.

Pavlides, S.B., Zhang, P., Pantosti, D., 1999. Earthquake, active faulting, and paleoseismological studies for the reconstruction of the seismic history of faults. Tectonophysics 308 (1–2), vii–x.

Rundle, J.B., Klein, W., Turcotte, D.L., Malamud, B.D., 2000. Precursory seismic activation and critical-point phenomena. Pure and Applied Geophysics 157, 2165–2182.

Stanley, H.E., 2003. Statistical physics and economic fluctuations: do outliers exist? Physica A 318 (1–2), 279–292.

Takayasu, H., 1990. Fractals in the Physical Science (Nonlinear Science: Theory and Application Series). Manchester University Press, Manchester. 180pp.

Tsunogai, U., Wakita, H., 1995. Precursory chemical changes in ground water; Kobe earthquake, Japan. Science 269 (5520), 61–63.

Turcotte, D.L., 1999. Seismicity and self-organized criticality. Physics of the Earth and Planetary Interiors 111 (3–4), 275–293.

Tzanis, A., Vallianatos, F., 2003. Distributed power-law seismicity changes and crystal deformation in the SW Hellenic ARC. Natural Hazards and Earth System Sciences 3, 1–17.

Uritsky, V.M., Pudovkin, M.I., Steen, A., 2001. Geomagnetic substorms as perturbed self-organized critical dynamics of the magnetosphere. Journal of Atmospheric and Solar-Terrestrial Physics 63 (13), 1415–1424.

Vespignani, A., Zapperi, S., 1998. How self-organized criticality works: a unified mean-field picture. Physical Review E 57 (6), 6345–6362.